Delocalization of disturbances and the stability of ac electricity grids

Stefan Kettemann

Department of Physics and Earth Science, Jacobs University, Campus Ring 1, 28759 Bremen, Germany and Division of Advanced Materials Science Pohang University of Science and Technology (POSTECH) San 31, Hyoja-dong, Nam-gu, Pohang 790-784, South Korea

(Received 24 April 2015; revised manuscript received 12 August 2015; published 21 December 2016)

In order to study how local disturbances affect the ac grid stability, we start from nonlinear power balance equations and map them to complex linear wave equations. Having obtained stationary solutions with phases φ_i at generator and consumer nodes i, we next study the dynamics of deviations. Starting with an initially localized perturbation, it is found to spread in a periodic grid diffusively throughout the grid. We find the parametric dependence of diffusion constant D. We apply the same solution strategy to general grid topologies and analyze their stability against local perturbations. The perturbation remains either localized or becomes delocalized, depending on grid topology, power capacity, and distribution of consumers and generator power P_i. Delocalization is found to increase the lifetime of perturbations and thereby their influence on grid stability, whereas localization results in an exponentially fast decay of perturbations at all grid sites. These results may therefore lead to new strategies to control the stability of electricity grids.

DOI: 10.1103/PhysRevE.94.062311

I. INTRODUCTION

The stability of electricity grids requires protecting them against perturbations [1–3]. Therefore, electrical power systems must be constructed in such a way that a physical disturbance does not result in exceeding bounds of system variable fluctuations. The energy transition towards an increased supply of decentralized renewable energy necessitates studying consequences of such structural changes for the stability of electricity grids and finding efficient ways to modify them to ensure their stability [4]. Since this is a highly complex and nonlinear problem, the study of its dependence on network topology, operating conditions, and forms of disturbances requires making modeling assumptions [2]. Recently, the synchronization of rotor angles in electricity grids has been modeled by a network of nonlinear oscillators [5–9]. Here, networks of generators and engines are described by a system of coupled differential equations for local rotor angles of generators and loads φ_i, where i's are grid nodes. The numerical solution of these differential equations showed that, on one hand, networks become more unstable with increasing decentralization against perturbations on short time scales with large amplitude, whereas the danger of a blackout can be reduced by decentralization [6]. In this article, we study how phase perturbations evolve with time in ac grids. The origin of such phase perturbations may arise, for example, due to local fluctuations in generating power from a wind generator. We start by finding stationary solutions for the spatial distribution of phase φ_i for a given distribution of active and reactive power, P_i and Q_i at the grid nodes i. Next, we reconsider the nonlinear dynamic power balance equations. For small deviations from the stationary solutions, we derive a linear wave equation describing the phase perturbation dynamics. Solving these equations, we explore how a local phase perturbation propagates with time through the grid. Depending on the geographical distribution of power, grid power capacity, and topology we find that it may either spread diffusively or become localized. This phenomenon generally is known as Anderson localization [10] where the coherent scattering of waves in a random medium causes their localization.

II. STEADY STATE POWER FLOW IN AC TRANSMISSION GRIDS

The power balance equations in ac transmission grids are obtained from Kirchhoff's laws at node i as

$$S_i = \sum_j V_i \left(\frac{V_i - V_j}{Z_{ij}} \right)^*, \tag{1}$$

where $S_i = P_i + iQ_i$. P_i is the active power produced at generator nodes $P_i > 0$ or consumed at consumer nodes $P_i < 0$, satisfying the total power balance condition $\sum_{i=1}^{N} P_i = 0$ with N as the total number of nodes. V_i is the voltage at node i. In an ac grid the reactive power Q_i of consumers is given while the one of generators is adjusted [3,11]. The transmission line from node i to j has impedance Z_{ij}. Neglecting small losses due to Joule's heat, we assume them to be purely inductive $Z_{ij} = i\omega L_{ij}$, where L_{ij} is the transmission line inductance between nodes i and j and ω is the grid frequency. Then, the voltage at node i is $V_i = V \exp(i\varphi_i)$, where V is fixed to nominal grid voltage and the power capacity of a transmission line is $K_{ij} = V^2/(\omega L_{ij})A_{ij}$, where A_{ij} is the adjacency matrix of the grid. Note that only $N-1$ phase angles φ_i remain to be determined as a function of the distribution of power P_i at N nodes constrained by the total power balance condition so that reactive power Q_i is fixed at all nodes. Defining $\psi_i^0(t) = \exp[-i\varphi_i^0(t)]$ with $\varphi_i^0(t) = \omega t + \theta_i^0$, phase angle θ_i^0 at node i in the steady state, it is convenient to write Eq. (1) as a linear wave equation,

$$S_i \psi_i^0(t) = \sum_j i K_{ij} \left[\psi_i^0(t) - \psi_j^0(t) \right]. \tag{2}$$

III. PHASE DYNAMICS

Phase dynamics in ac electricity grids has been modeled by active power balance equations with additional terms describing the dynamics of rotating machines [5–7,11–14]. One term describes the inertia to changes in the kinetic energy of a synchronous rotating generator or motor with rotor angle

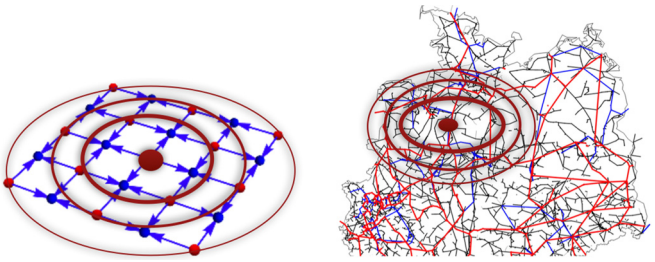

FIG. 1. Left: square grid of generators (red) and consumers (blue). Arrows: direction of active power transmission F. Right: topology of German transmission [380 kV (red), 220 kV (blue)], and high voltage distribution grid [110 kV (black)] [16]. A propagating disturbance is sketched as red circles.

φ_i with inertia J when we assume that all loads are either synchronous or induction motors, whose dynamics can be modeled that way [3]. Another term describes the damping with coefficient γ. Adding these terms to the active power balance equations, the real part of Eq. (1) yields for purely inductive transmission lines [5,6,11–14],

$$P_i = \left(\frac{J}{2}\frac{d}{dt} + \gamma\right)\left(\frac{d\varphi_i}{dt}\right)^2 + \sum_j K_{ij}\sin(\varphi_i - \varphi_j). \quad (3)$$

We note that for fixed voltage V there are no dynamic terms in the reactive power balance equation, which appear only in higher order when voltage dynamics in addition to the phase dynamics are considered [15].

IV. DYNAMICS OF DISTURBANCES IN THE GRID

In order to study the propagation of disturbances, such as fluctuations in power supply $\delta P(t)$ or in power capacitance δK_{ij}, we set $\varphi_i(t) = \omega t + \theta_i^0 + \alpha_i(t)$ with steady state phases θ_i^0, the solutions of Eq. (2). We study the dynamics of phase disturbances $\alpha_i(t)$ which are governed by

$$\partial_t^2\alpha_i + 2\Gamma\,\partial_t\alpha_i = \frac{P_i}{J\omega} - \sum_j \frac{K_{ij}}{J\omega}\sin\left(\theta_i^0 - \theta_j^0 + \alpha_i - \alpha_j\right), \quad (4)$$

where $\Gamma = \gamma/J$. Considering small perturbations from the stationary state ψ_i^0, we expand Eq. (4) in $\alpha_i - \alpha_j$, yielding linear wave equations on the grid,

$$\partial_t^2\alpha_i + 2\Gamma\,\partial_t\alpha_i = -\sum_j t_{ij}(\alpha_i - \alpha_j), \quad (5)$$

with hopping amplitude $t_{ij} = K_{ij}\cos(\theta_i^0 - \theta_j^0)/(J\omega)$. Note that t_{ij} depends both on power capacitance K_{ij} and thereby the grid topology as well as on the initial distribution of power P_i through the stationary phases θ_i^0. With $\alpha_i(t) = \sum_n c_{ni}\exp(-i\omega_n t)$ we get for $\Gamma = 0$ the spectral representation of the linear wave equation,

$$\omega_n^2 c_{ni} = \sum_j t_{ij}(c_{ni} - c_{nj}), \quad (6)$$

with eigenfrequencies ω_n and eigenmodes c_n. $c_0 = 0$, $\omega_0 = 0$ correspond to the stationary solution. For $\Gamma \neq 0$ we get from Eq. (5) the same eigenmodes c_n with complex eigenfrequencies $\Omega_n = -i\Gamma + i\sqrt{\Gamma^2 - \omega_n^2}$. Equation (6) can be solved for arbitrary electricity grids, such as the German transmission grid shown in Fig. 1 (right) where the hopping matrix elements t_{ij} with stationary phases θ_i^0 are obtained from the solution of Eq. (2).

V. SQUARE GRID

As an example, let us first consider a grid where all transmission lines have equal length a. We start with a periodic arrangement of generators and consumers as shown for a square grid in Fig. 1 (left). Assuming that all generators on sublattice G generate power $P_{\mathbf{x}} = +P$, $\mathbf{x} \in G$ while all consumers on sublattice C consume power $P_{\mathbf{x}} = -P$, $\mathbf{x} \in C$, we find the solution by making the Bloch ansatz for the stationary solution,

$$\begin{aligned}\psi_k(\mathbf{x} \in G, t) &= \psi_{Gk}e^{i\mathbf{k}\cdot\mathbf{x}}\exp(-i\omega t),\\ \psi_k(\mathbf{x} \in C, t) &= \psi_{Ck}e^{i\mathbf{k}\cdot\mathbf{x}}\exp(-i\omega t),\end{aligned} \quad (7)$$

where $\mathbf{k}$ is a wave number. For periodic boundary conditions on the grid of linear size L in all d directions with unit vectors $\hat{e}_n$, $n = 1,\ldots,d$, $\psi_k(\mathbf{x} + L\hat{e}_n) = \psi_k(\mathbf{x})$, for all $n = 1,\ldots,d$, the wave number is $\mathbf{k} = 2\pi\mathbf{n}/L$ where the components of the vector $\mathbf{n}$, $n_n, n = 1,\ldots,d$ are integers. For each wave number $\mathbf{k}$ we find a solution of the form Eq. (7) where the phase factors ψ_{Gk}, ψ_{Ck} are given by

$$\psi_{Ck} = \exp(i\delta_k)\psi_{Gk}, \quad \text{with } \sin\delta_k = P/(f_k K), \quad (8)$$

where $f_k = 2\sum_{n=1}^d \cos(k_n a)$ depends on wave number components k_n. For given reactive power Q, which is for this arrangement of consumers and generators constrained by Eq. (2) to be the same at all nodes, the wave vector $\mathbf{k}$ is determined by the equation,

$$f_k^2 = (Q/K - 2d)^2 + P^2/K^2. \quad (9)$$

The transmitted power between sites i and j is $F_{ij} = iK_{ij}[\psi_i(t) - \psi_j(t)]\psi_i(t)^*$. For the homogenous state $\mathbf{k} = 0$ the active power transmitted between neighbored sites $i \in G$ and sites $j \in C$ is $\mathrm{Re}\,F_{ij} = P/(2d)$ as shown in Fig. 1 (left) on a square lattice where arrows indicate the direction of active power transmitted from generators to neighbored consumers. The reactive power in the transmission lines is $\mathrm{Im}\,F = K(1 - \sqrt{1 - \frac{P^2}{4d^2K^2}})$, which is for $P \ll K$ much smaller than the transmitted active power. For finite wave vector $\mathbf{k}$ the active power transmitted between $i \in G$ and $j \in C$ for $\mathbf{k} = k\hat{e}_n$ is $\mathrm{Re}\,F_{ij} = K\,\sin(\delta_k \pm k_n a)$ with a unit vector between i and j, $\hat{e}_{ij} = \pm\hat{e}_n$. In all other directions $\mathrm{Re}\,F_{ij} = K\,\sin\delta_k$.

VI. STABILITY

Disregarding the dependence of α_i on the perturbation at neighbored sites α_j reduces Eq. (4) to the one of a damped driven nonlinear pendulum. For long times $t \gg 0$ it has two stable solutions: *(1) Stationary solution* $\partial_t\alpha_i = 0$, $\alpha_i = n2\pi$, n integer, to which small deviations decay exponentially. *(2) Overswinging pendulum solution* when the driving force and damping are in balance. The phase velocity converges then to

$$\partial_t\alpha_i(t) = \Omega_i - \sum_j \frac{K_{ij}\sin\left(\Omega_i t + \theta_i^0 - \theta_j^0 + \eta_i\right)}{J\omega\sqrt{\Omega_i^2 + 4\Gamma^2}}, \quad (10)$$

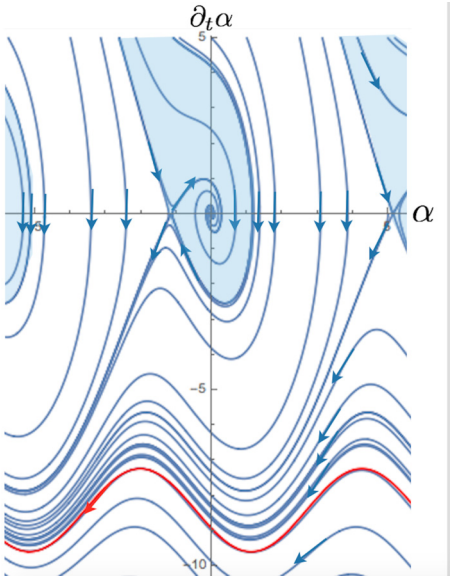

FIG. 2. Phase curves of Eq. (4) for α_i, setting $\alpha_j = 0$. Flow directions are indicated by arrows. Stable fixed points are $\alpha_i = n2\pi$, $\partial_t\alpha_i = 0$. Separatrices are $\alpha_{il} = 2\delta_k + (2l+1)\pi$, $\partial_t\alpha_i = 0$. The blue shaded areas are basins of attraction. All other phase points converge to Eq. (10) (red curve).

with frequency $\Omega_i = P_i/(2\Gamma J\omega)$ and phase shift $\eta_i = \arctan(2\Gamma/\Omega_i)$. In Fig. 2 phase curves are shown for the square lattice with $\theta_i^0 - \theta_j^0 = \pm\delta_k + k_n a$. Regions of stability are shaded in blue, outside which all phase points converge to open orbit solution Eq. (10) (red). A condition for phase points to lie inside the stability region is obtained by approximating its irregular shape by an ellipse whose vertex on the α axis is given by the saddle point $\alpha_{il} = 2\delta_k - \pi$. Its vertex on the $\partial_t\alpha$ axis is given by a linear interpolation of stable trajectory on the separatrix $\partial_t\alpha = -(\pi - 2\delta_k)\Gamma\lambda$, where $\lambda = -1 - \sqrt{1 + \frac{2dK\cos(\delta_k)}{J\omega\Gamma^2}}$. Thus, phase points are inside the basin of attraction if they satisfy

$$\alpha_i^2 + \frac{(\partial_t\alpha_i)^2}{\Gamma^2\lambda^2} \ll (\pi - 2\delta_k)^2. \tag{11}$$

VII. PROPAGATION OF LOCAL DISTURBANCES

Now, we can study the propagation of disturbances in a square grid by inserting the analytical steady state solutions Eqs. (7)–(9) into the dynamical equations Eq. (4). If we perturb the phase at node $i = n$, $\alpha_n(t=0) = \alpha_0 \neq 0$, whereas $\alpha_i(0) = 0$ at all other nodes $i \neq n$, that disturbance excites nodes $i \neq n$ at later times $t > 0$. For a small perturbation, satisfying Eq. (11), we can use linearized wave equations Eq. (5) with $t_{ij} = K_{ij}\cos\delta_k/(J\omega)$. Using the spectral representation $\alpha_i(t) = \sum_q c_q e^{i\mathbf{q}\cdot\mathbf{r}_i} e^{-i\epsilon_q t}$, insertion into Eq. (5) gives the complex frequency,

$$\epsilon_q = -i\Gamma\left[1 \pm \sqrt{1 - \frac{2dK\cos\delta_k}{J\omega\Gamma^2}\left(1 - \frac{f_q}{2d}\right)}\right]. \tag{12}$$

For finite Γ and small q the dispersion is quadratic $\epsilon_q = -i\frac{Ka^2\cos\delta_k}{J\omega\Gamma}\mathbf{q}^2$. For large momenta q, the ballistic limit,

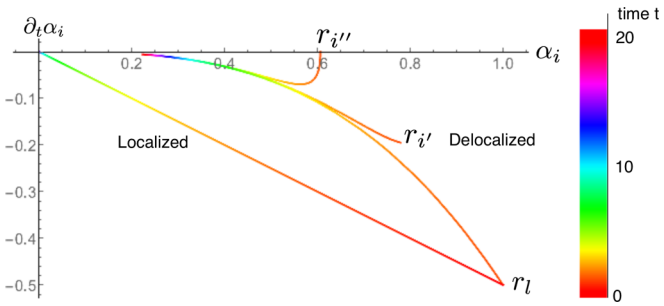

FIG. 3. Phase curves at initial site r_l and other sites $r_{i'}$,$r_{i''}$. Time progresses as indicated on the color bar in units of $\tau = 1/\Gamma$. Delocalization causes slow decay of the perturbation at the initial site and an initial increase, followed by a slow decay at other sites (upper curves). Localization causes an exponentially fast decay at all sites (lower curve).

the dispersion is linear $\epsilon_q|_{\Gamma=0} = v_k q$ with velocity $v_k = \sqrt{K\cos\delta_k/(J\omega)}a$. An initially localized perturbation, $c_q = \text{const.}$ becomes for times $t > \tau = 1/\Gamma$ and distances exceeding the mean free path $l = v\tau$, $|r_i - r_l| > l$,

$$\alpha_i(t) = \frac{\alpha_0}{(4\pi D_k t/a)^{d/2}}\exp\left(-\frac{(\mathbf{r}_i - \mathbf{r}_l)^2}{4D_k t}\right). \tag{13}$$

Thus, the initially localized perturbation spreads diffusively with diffusion constant,

$$D_k = \frac{Ka^2\cos\delta_k}{\omega\gamma} = \frac{v_k^2\tau}{2}, \tag{14}$$

as shown in Fig. 3 where $\partial\alpha_i$ is plotted versus phase perturbation α_i at initial site $i = l$ and other sites i',i'' for diffusive times $t > \tau = 1/\Gamma$ using Eq. (13). Time is progressing as indicated on the color bar in units of τ. Diffusion causes slow decay of the perturbation at the initial site and an initial increase, followed by a slow decay at other sites. The area A_t where nodes become perturbed at time t, increases diffusively with time as $A_t = D_k t$. In order to quantify the stability with Eq. (11) we calculate the spatial average $\delta\alpha = \sqrt{\frac{1}{N}\sum_i \alpha_i^2} = \frac{\alpha_0}{(8\pi D_k t/a)^{d/4}}$, $\delta\omega = \sqrt{\frac{1}{N}\sum_i \left(\frac{d\alpha_i}{dt}\right)^2} = \frac{\sqrt{d(2+d)}}{4t}\delta\alpha$, decaying with a power law in time.

For power capacity $K = 0.5$ GW, $d = 2$, grid frequency $\omega = 2\pi 50/s$, power $P = 1.9$ GW, inertia $J = 10^5$ kg m^2, and damping $\Gamma = 1/s$ the perturbation spreads initially with velocity $v = 2.22a/s$. Beyond mean free path $l = 2.22a$ it spreads diffusively with diffusion constant $D_0 = 2.46a^2/s$. The time to diffuse a length $L = 10a$ is $t_D = L^2/D_0 = 40.64$ s. The closer power P is to capacity limit $K_c = 2dK$, the smaller is diffusion constant D, the longer survives the disturbance.

The propagation of any type of disturbance can be studied with Eq. (4). For example, a change in power δP at $t_0 = 0$ at neighbored nodes i,j, $\delta P_i = -\delta P_j = \delta P$ changes transmitted power between nodes k,l at time t,

$$\delta F_{kl}(t) = \pm\delta P\, A_{kl}\frac{\pi^2 a^2}{\omega_0 D_k t^2}\exp\left(-\frac{(\mathbf{r}_i - \mathbf{r}_l)^2}{4D_k t}\right), \tag{15}$$

with $+$ when k is a generator and l is a consumer and $-$ vice versa. Similarly, the change in power flow due to a static perturbation $\delta P_i = -\delta P_j = \delta P$ is given by

$$\delta F_{kl} = \pm\delta P\, A_{kl} 2\pi a^2/(\mathbf{r}_i - \mathbf{r}_l)^2. \tag{16}$$

An instantaneous change in power capacitance $\delta K\ A_{ij}$ causes a change in power Eqs. (15) and (16) for a static perturbation, replacing δP by δK, respectively.

VIII. LOCALIZATION OF DISTURBANCES

Equation (6) can be applied to study the propagation of disturbances in ac grids of arbitrary distribution of power P_i, arbitrary grid topology, and power capacity K_{ij} by calculating the hopping amplitude $t_{ij} = K_{ij}\cos(\theta_i^0 - \theta_j^0)/(J\omega)$ from the steady state solutions θ_i^0 as found by solving Eq. (2). In a first attempt to model the complexity of a real grid, we take a random distribution of t_{ij} caused by the wide distribution of power P_i and the real grid topology with its complex network structure. Equation (6) first appeared in the problem of randomly coupled atoms in harmonic approximation. For chains it has been solved for various random distributions of t_{ij} [17–20]. If t_{ij} is taken from a box distribution, the density of eigenmodes is constant $\rho(\Omega_n) = 1/\omega$ for $0 < \Omega_n < \omega$. For nonzero Ω_n the eigenstates are localized with localization length $\xi(\Omega_n) \sim 1/\Omega_n$ [17–20]. The localization length of the lowest eigenfrequency $\Omega_1 \sim \omega a/L$ is long, on the order of the system size $\xi_1 \sim L$. The highest eigenfrequency $\Omega_n \to \omega$ has a localization length $\xi \to 2a$, twice the length a of a transmission line. In dimension $d = 2$, which is the situation most relevant for real grids, all eigenstates remain localized for nonzero Ω_n, but the localization length can be for small Ω_n exponentially large so that it typically is larger than the system size for realistic grid extensions L. This might explain that in Ref. [21] we found in square grids a long range power law decay with power $q = 2$ as in Eq. (16), even when taking a random distribution of P_i. Also in a real grid topology we found long range decay [21]. Typically, the localization length is smallest in treelike grids, while it becomes longer, the more meshed the grid becomes. In dimensions $d > 2$, there is a critical value ω_c such that for $\omega_n > \omega_c$ all modes are localized, whereas they are extended for $\omega_n < \omega_c$ [20,22]. If the phase perturbation is initially in a state localized around site r_0 with localization length ξ_n, it decays in time t as $\alpha_i(t) = \alpha_0 \exp(-\frac{|r_i - r_0|}{\xi_n})\exp(-\tilde{\Gamma}_n t)$, where $\tilde{\Gamma}_n = \mathrm{Re}[\Gamma - \sqrt{\Gamma^2 - \omega_n^2}]$. The typical phase and frequency shifts are found to decay exponentially fast as

$$\delta\alpha = \alpha_0\sqrt{\xi_n/a}\exp(-\tilde{\Gamma}_n t), \quad \delta\omega = \tilde{\Gamma}_n\delta\alpha. \tag{17}$$

Thus, localization causes exponentially fast decay of phase perturbations at all nodes i as shown in Fig. 3 where it is compared with a delocalized phase perturbation decaying with a power in time t Eq. (13).

IX. CONCLUSIONS

Local perturbations, arising, for example, from power fluctuations, are found to spread diffusively in a periodic grid, decaying slowly with a power law in time and space. The closer the generator power P comes to the capacity limit K_c, the smaller the diffusion constant D, the longer the perturbation takes to decay. Modeling the complexity of a realistic grid with a random distribution of generators and consumers and/or random transmission power capacity the phase perturbation is found to become localized in one- and two-dimensional grids. Localization leads to an exponentially fast decay of phase perturbations at all sites, whereas delocalization results in diffusive slow decay, Fig. 3. Initially small perturbations may then add up at some nodes to large perturbations and push the system outside of the region of stability. We conclude that it is favorable for stable grid operation to ensure that phase perturbations remain localized, decaying exponentially fast at all sites. The consequences of these results for real electricity grid topologies will be studied by solving Eqs. (2) and (6) numerically in a future publication. We also plan to study how the spreading of perturbations is modified when including voltage fluctuations using, for example, the third order model [1,3,7]. Although we assumed here a network of synchronous generators and motors, modern wind turbines are rather induction generators, the most modern ones being the doubly fed induction generator, converting the power from ac to dc and then to ac with the grid frequency [3]. Thus, the energy transition towards an increased supply of decentralized renewable energy necessitates getting a better understanding of how the dynamic equations are modified and understanding the resulting consequences for the grid dynamics.

ACKNOWLEDGMENTS

We thank M. Rohden for stimulating discussions and D. Jung for useful comments. We gratefully acknowledge support from BMBF CoNDyNet FK Grant No. 03SF0472A.

[1] P. Kundur, *Power System Stability and Control* (McGraw-Hill, New York, 1994).
[2] P. Kundur *et al.*, IEEE Trans. Power Syst. **19**, 1387 (2004).
[3] J. Machowski, J. W. Bialek, and J. R. Bumby, *Power System Dynamics: Stability and Control*, (Wiley, Hoboken, NJ, 2008).
[4] S. M. Amin, A. M. Giacomoni, in *Fundamentals of Materials for Energy and Environmental Sustainability*, Edited by D. S. Ginley and D. Cahen (Cambridge University Press, Cambridge, U.K., 2011).
[5] A. R. Bergen and D. J. Hill, IEEE Trans. Power Appar. Syst. **PAS-100**, 25 (1981).
[6] M. Rohden, A. Sorge, M. Timme, and D. Witthaut, Phys. Rev. Lett. **109**, 064101 (2012).
[7] K. Schmietendorf, J. Peinke, R. Friedrich, and O. Kamps, Eur. Phys. J.: Spec. Top. **223**, 2577 (2014).
[8] M. Rohden, A. Sorge, D. Witthaut, and M. Timme, Chaos **24**, 013123 (2014).
[9] D. Manik, D. Witthaut, B. Schäfer, M. Matthiae, A. Sorge, M. Rohden, E. Katifori, and M. Timme, Eur. Phys. J.: Spec. Top. **223**, 2527 (2014).
[10] P. W. Anderson, Phys. Rev. **109**, 1492 (1958).
[11] K. Heuck, K.-D. Dettmann, and D. Schulz, *Elektrische Energieversorgung* (Springer, Wiesbaden, 2013).
[12] G. Filatrella, A. H. Nielsen, and N. F. Pedersen, Eur. Phys. J. B **61**, 485 (2008).
[13] M. Rohden, Ph.D. thesis, Göttingen, 2014.

[14] P. J. Menck, J. Heitzig, J. Kurths, and H. J. Schellnhuber, Nat. Commun. **5**, 3969 (2014).
[15] Reactive power balance dynamics is directly coupled to voltage dynamics [1,3,7].
[16] S. Tamrakar, B.S. thesis, Jacobs University, 2015.
[17] F. J. Dyson, Phys. Rev. **92**, 1331 (1953).
[18] S. Alexander, J. Bernasconi, W. R. Schneider, and R. Orbach, Rev. Mod. Phys. **53**, 175 (1981).
[19] T. A. L. Ziman, Phys. Rev. Lett. **49**, 337 (1982).
[20] F. J. Wegner, in *50 Years of Anderson Localization*, edited by E. Abrahams (World Scientific, Singapore, 2010).
[21] D. Jung and S. Kettemann, Phys. Rev. E **94**, 012307 (2016).
[22] S. John, H. Sompolinsky, and M. J. Stephen, Phys. Rev. B **27**, 5592 (1983).